

Comparison of Seven Artificial Intelligence-Assisted Prediction Models for Renal Fibrosis in Chronic Kidney Disease Using Aggregate Index of Systemic Inflammation and Ultrasound Radiomics

Yutao Wu^{1,*}, Kun Lu^{1,*}, Yixiang Liao², Jing Wang¹, Tao Yang², Li Wang², Fei Li¹

¹Department of Urology, The Second Hospital of Jingzhou, Jingzhou, Hubei, People's Republic of China; ²Department of Urology, Jingzhou Hospital Affiliated to Yangtze University, Jingzhou, Hubei, People's Republic of China

*These authors contributed equally to this work

Correspondence: Fei Li, Email lwf0070@163.com

Objective: Renal fibrosis, key in progressive chronic kidney disease (CKD), requires invasive biopsy for diagnosis. This study aimed to develop an optimized artificial intelligence (AI)-assisted model for pre-biopsy screening.

Methods: A multicenter retrospective study included 758 renal fibrosis patients from two tertiary hospitals. 515 from The Second Hospital of Jingzhou were split 7:3 into training and internal validation sets; 243 formed an external test set. Severity (mild/moderate-to-severe) was classified via Banff score. Convolutional neural networks (CNN) extracted features from renal ultrasound images; peripheral blood counts were collected. After Least Absolute Shrinkage and Selection Operator (LASSO) variable screening, machine learning (ML) models were built, evaluated via receiver operating characteristic (ROC) curve's area under the curve (AUC) and decision curve analysis (DCA).

Results: The model combining ultrasound radiomics and Aggregate Index of Systemic Inflammation (AISI) showed AUC 0.71–0.96 in training/internal validation, 0.89 in external test. Random Forest (RF) performed best (AUC 0.96 in training; 0.93/0.95 in internal/external validation).

Conclusion: The RF-based model effectively evaluates renal fibrosis in CKD patients. Integrating AISI and ultrasound radiomics offers a novel strategy for dynamic assessment and biopsy guidance.

Keywords: chronic kidney disease, artificial intelligence, renal fibrosis, machine learning, aggregate index of systemic inflammation, predictive model

Introduction

In the past few decades, the global age-specific mortality rate of chronic kidney disease (CKD) has continued to rise, affecting approximately 9.1% of the global population and imposing a heavy burden on patients and healthcare.^{1,2} CKD has always been an established risk of cardiovascular disease, and timely diagnosis can help prevent adverse outcomes such as end-stage renal disease and related cardiovascular diseases.^{3,4} Specifically, in various stages of CKD, the extracellular matrix undergoes renal interstitial fibrosis and tubular atrophy (IF/TA), which is negatively correlated with renal function.^{5–7} Therefore, timely assessment of CKD progression through IF/TA testing is necessary. Up to now, glomerular filtration rate is commonly used to evaluate renal function in CKD patients, but it cannot accurately reflect renal function and is easily influenced by the population. In addition, although percutaneous renal biopsy is the “gold standard” for diagnosing and understanding renal fibrosis changes, it is not suitable for long-term monitoring of disease progression and evaluation of treatment effectiveness.⁸ Given this, it is extremely urgent to non-invasively and accurately detect and monitor the degree of TA/IF in the kidneys of CKD patients to assist clinicians in evaluating the progression of fibrosis caused by CKD.

Ultrasound imaging is a commonly used diagnostic method for evaluating CKD in clinical diagnosis and treatment.^{9–11} Although there may be texture information in ultrasound images that cannot be observed with the naked eye, it can be obtained through radiomics. In recent years, radiomics has used computer technology to extract texture features and high-dimensional image features from ultrasound images to quantify image information, which are correlated with biological and pathological information.^{12,13} At present, radiomics in the field of kidney has found that wavelet transform based features in ultrasound radiomics are of great significance for distinguishing CKD kidneys from healthy kidneys, and ultrasound radiomics can be used to evaluate the degree of renal function damage in CKD.^{14–16} However, the feature extraction of ultrasound imaging omics and optimization of advanced machine learning (ML) algorithms are still ongoing, providing alternative diagnostic strategies for non-invasive diagnosis of renal fibrosis. Encouraged by this, we hope to use convolutional neural networks to extract ultrasound image parameters more widely in this study, and use artificial intelligence algorithms to construct a kidney fibrosis prediction model with better predictive performance.

As a biomarker for evaluating systemic inflammation, the Aggregate Index of Systemic Inflammation (AISI) was initially designed to assess the inflammatory status of patients with idiopathic pulmonary fibrosis (IPF), primarily by reflecting the ratio of immune cell subsets (such as neutrophils, lymphocytes, and monocytes) to platelet count to evaluate systemic inflammatory response.^{17,18} The advantages of AISI include low cost, easy collection, and simple calculation, making it potentially valuable for clinical applications. At present, some scholars have found that AISI is a more comprehensive inflammatory indicator than SII and SIRI, which can more comprehensively evaluate the systemic inflammatory status, especially in evaluating proteinuria.^{19–21} With the help of NHANES, the relationship between AISI and CKD or low eGFR has been confirmed.²² However, the potential role of AISI in kidney disease (especially renal fibrosis) still needs further clinical research to verify.

Therefore, this study collected a large sample size of clinical data and attempted to construct a clinical ML prediction model based on renal ultrasound radiomics and AISI to evaluate the degree of fibrosis in CKD, providing clinicians with a low-cost and efficient method for evaluating the degree of fibrosis.

Materials and Methods

Study Population

We retrospectively collected 758 patients diagnosed with CKD at the Second Hospital of Jingzhou and Jingzhou Hospital Affiliated to Yangtze University from January 2017 to July 2024. The inclusion criteria are as follows: (1) Diagnosis of CKD through percutaneous renal biopsy; (2) Optical microscope specimens >10 glomeruli; (3) Age >18 years old; (4) Ultrasound examination should be performed within 3 days before the patient's renal puncture surgery. Exclusion criteria: (1) Acute kidney injury and heart valve disease; (2) Renal artery stenosis or urinary tract obstruction; (3) Cysts or tumors; (4) Ultrasound images are missing or of poor quality.

Percutaneous renal biopsy was performed by two experienced ultrasound physicians, both of whom selected the left kidney for biopsy. According to the distribution range of IF/TA in the glomerular cortex, patients are divided into three categories: TA/IF₀, 0–25%; TA/IF₁, 26%–50%; TA/IF₂ >50%. Due to the small number of TA/IF class 2 patients, they were not included in this study. The construction process of patient inclusion and prediction models was detailed in Figure 1.

Ethical Statement

This study was approved by the Ethics Committee of the Second Hospital of Jingzhou. Due to its retrospective nature, involving de-identified existing medical records, the Committee waived the requirement for individual patient consent, as the research posed minimal risk and obtaining consent was impracticable. Strict confidentiality measures were applied, all records were anonymized, access was restricted to the research team, and data handling complied with relevant privacy regulations to prevent patient identification. This study was conducted in accordance with the principles of the Declaration of Helsinki (World Medical Association, 2013 revision) for medical research involving human subjects.

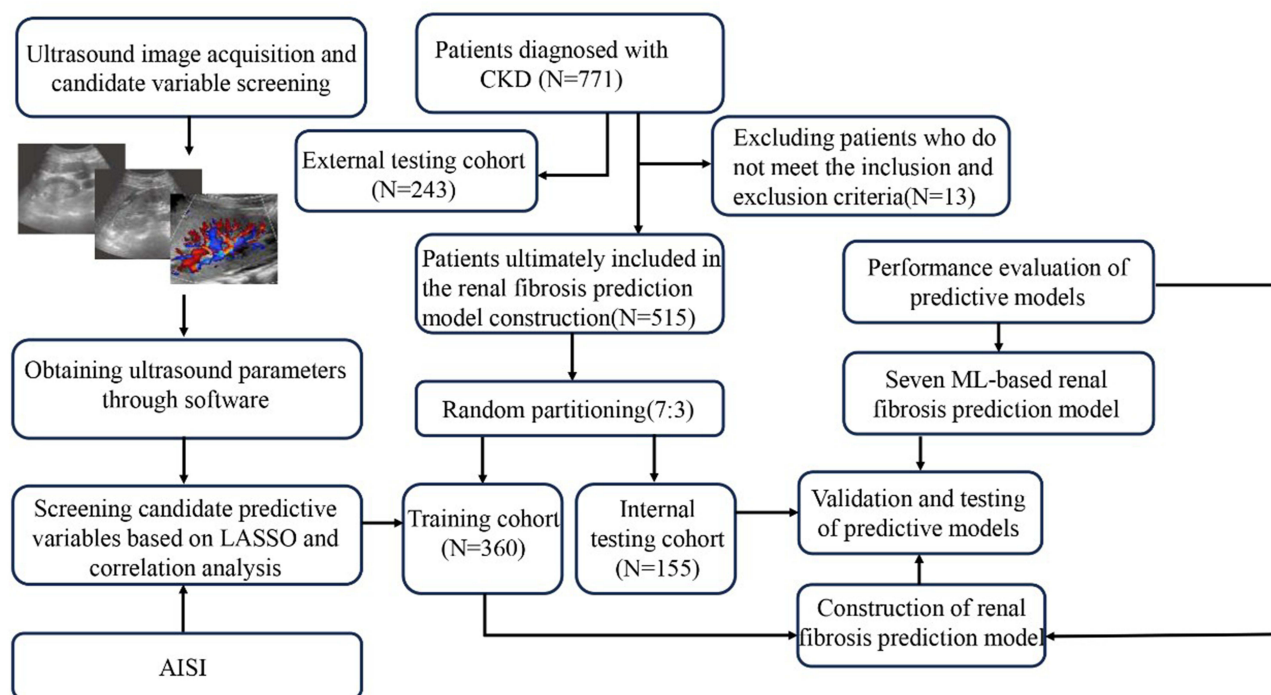


Figure 1 Workflow diagram for patient inclusion and prediction model establishment.

Data Collection

We collected demographic data (age, gender, body mass index[BMI], etc.), laboratory tests (blood routine, liver and kidney function electrolytes, coagulation function, etc.), and ultrasound image information of patients from standardized sources such as electronic health records in hospitals. Other clinical data: gender, age, mean arterial pressure, hemoglobin, platelet count, creatinine eGFR1, Urea, uric acid, 24-hour urine protein, 24-hour urine volume. All data collection was independently entered and verified by two professionals. To ensure the accuracy and verifiability of the entered data, we used Epidata software for programming and input. Finally, a third-party professional performed final verification and data cleaning on the entered data.

Ultrasound Radiomics Feature Extraction

Two ultrasound doctors with over 5 years of experience in abdominal ultrasound examination use ITK 3.8.0 software (<http://www.itksnap.org/>) to outline the region of interest (ROI) of renal ultrasound images and perform manual segmentation (2×2 cm²), image resolution (512×512 pixels), and CNN architecture (12 layers with ReLU activation). Next, we randomly selected renal ultrasound images of patients and had two doctors independently perform ROI delineation. After 2 weeks, we repeated the same steps to evaluate the matching degree of feature extraction, while retaining features with good correlation for subsequent analysis. Finally, we used PyRadiomics 3.0.1 online analysis tool to automatically extract and quantify the features of ultrasound.

Construction of ML-Based Prediction Models

As shown in [Figure 1](#), the features with intra group correlation coefficient (ICC)>0.75 in the training queue were retained. Then, single factor logistic regression analysis was used to screen out the features with significant differences between IF/TA class 0 and class 1 in the training group. Finally, the minimum absolute shrinkage and selection operator algorithm was used to select the optimal features, and the ML algorithm was used to establish an ultrasound radiomics prediction model.

Evaluation of ML-Based Predictive Model Performance

In this study, we used seven ML algorithm prediction models, namely extreme gradient boosting (EGE), support vector machine(SVM), random forest(RF), multilayer perceptron(MLP), artificial neural network(ANN), naive Bayes(NB), and generalized linear logistic regression(GLR), to construct prediction models. The 10-fold cross validation was used to ensure the stability of the model. We evaluated the performance of the prediction model based on the AUC, sensitivity, specificity, recall, F1 score, accuracy, and of the ROC curve. Additionally, we also plotted decision curve analysis (DCA) and calibration curves to demonstrate its true clinical use. To determine the optimal threshold probability of our model, we generated a Clinical Impact Curve (CIC) for rigorous evaluation and determination of the most effective clinical application decision threshold.

Statistical Analysis

We used SPSS 25.0 and R software (version 4.3.2). Metric data that follows a normal distribution are represented by mean \pm standard deviation, metric data that does not follow a normal distribution are represented by M (Q1, Q3), and count data are represented by example (%). The *t*-test, Mann Whitney *U*-test, and chi square test were used for univariate analysis, while binary logistic regression analysis was used for multivariate analysis. We used Delong test to compare the differences in area under the curve (AUC) of each prediction model between the training group and the validation group. $P < 0.05$ indicates a statistically significant difference.

Results

Baseline Characteristics

A total of 758 patients diagnosed with CKD were included in the final study. Among them, a total of 135 patients were diagnosed with renal fibrosis through renal biopsy, accounting for approximately 17.8%. 515 patients were randomly divided into the predictive model training set and the internal test set at a ratio of 7 to 3(as shown in [Table 1](#)). In addition, as shown in [Supplementary Table 1](#), another 243 patients were considered as an external test set, of which 24.7% were diagnosed with renal fibrosis. In the comparison of baseline data between the renal fibrosis group and the non-renal fibrosis group, the results showed that there were no significant statistical differences in age, gender, BMI, etc. of the patients ($P > 0.05$). However, among the relevant indicators of laboratory examinations, there were significant statistical differences between groups in terms of neutrophil count(NEU), platelet count(PLT), monocyte count(MONO), and lymphocyte count(LYM), etc. ($P < 0.05$). The calculation formula of AISI is as follows: $AISI = \frac{NEU \times PLT \times MONO}{LYM}$. The results showed that there was a significant statistical difference in AISI between the renal fibrosis group and the non-renal fibrosis group ($P < 0.05$). The ultrasound radiomics parameters are mainly obtained from ultrasound images, including texture features, gray-scale matrix parameters, and ultrasound hemodynamic features, etc. We used the convolution kernel parameters and bias parameters of CNN to adjust the output range of convolution. Ultimately, we extracted 167 generalized ultrasound radiomics parameters. Among them, the parameters based on the gray matrix showed a significant statistical difference between the renal fibrosis group and the non-renal fibrosis group ($P < 0.05$). The ultrasound radiomics data were summarized in [Supplementary Table 2](#).

Selection of Candidate Predictor Variables

As shown in [Figure 2A](#), in the heat map of candidate predictor variables and outcomes (ie, renal fibrosis) constructed by Pearson correlation coefficient, the results indicated a significant positive correlation between AISI and renal fibrosis ($P < 0.05$), while based on the parameter characteristics extracted from ultrasound radiomics, For example, Angular Second Moment(ASM), Contrast, Correlation, Entropy, Inverse Difference Moment(IDM) were significantly correlated with renal fibrosis ($P < 0.05$). Then, as shown in [Figures 2B and C](#), the LASSO regression analysis results suggest that the optimal number of variables corresponding to the equation λ -se is 5. Therefore, we finally included 5 variables into the equation. Including AISI, ASM, Contrast, Correlation, Entropy, and IDM. In addition, for the weight value distribution of the candidate variables, we also sorted the weight values based on the SHAP interpretability algorithm, as shown in [Figure 2D](#). Based on the fact that the ultrasound radiomics parameters occupy a large weight proportion in all candidate variables, especially the ultrasound feature parameters

Table I Analysis of Baseline Data for Training and Internal Validation Sets

Variables	Training Set			P-value	Internal Testing Set			P-value
	Overall (n=360)	Renal Fibrosis (n=101)	Normal (n=259)		Overall (n=155)	Renal Fibrosis (n=34)	Normal (n=121)	
Sex (%)								
Male	179 (49.7)	54 (53.5)	125 (48.3)	0.441	83 (53.5)	15 (44.1)	68 (56.2)	0.292
Female	181 (50.3)	47 (46.5)	134 (51.7)		72 (46.5)	19 (55.9)	53 (43.8)	
Age (median [IQR]),year	56.00 [45.00, 65.00]	57.00 [43.00, 65.00]	56.00 [46.00, 65.00]	0.935	55.00 [44.00, 66.00]	58.00 [42.25, 67.75]	55.00 [44.00, 66.00]	0.998
BMI (median [IQR]),kg/m ²	24.50 [21.90, 27.33]	24.90 [22.20, 27.40]	24.20 [21.85, 27.30]	0.451	25.00 [22.15, 27.05]	25.25 [22.72, 26.45]	24.90 [22.00, 27.20]	0.733
Hypertension (%)								
Yes	160 (44.4)	42 (41.6)	118 (45.6)	0.573	73 (47.1)	13 (38.2)	60 (49.6)	0.328
No	200 (55.6)	59 (58.4)	141 (54.4)		82 (52.9)	21 (61.8)	61 (50.4)	
Diabetes (%)								
Yes	185 (51.4)	57 (56.4)	128 (49.4)	0.281	75 (48.4)	14 (41.2)	61 (50.4)	0.448
No	175 (48.6)	44 (43.6)	131 (50.6)		80 (51.6)	20 (58.8)	60 (49.6)	
eGFR (median [IQR]), mL/min/1.72 m ²	37.20 [23.45, 58.50]	76.10 [65.50, 88.60]	30.20 [20.55, 38.40]	<0.001	35.50 [22.35, 49.40]	72.90 [64.43, 88.12]	29.60 [20.10, 38.60]	<0.001
Cyst C (median [IQR]), mg/L	1.49 [1.04, 2.00]	1.46 [1.06, 1.87]	1.51 [1.04, 2.03]	0.586	1.49 [0.95, 2.08]	1.20 [0.86, 1.89]	1.54 [1.04, 2.08]	0.123
UTP (median [IQR]), g/d	4.00 [2.37, 5.81]	4.01 [2.38, 5.89]	3.97 [2.36, 5.80]	0.958	4.16 [2.46, 5.64]	4.75 [3.35, 6.19]	3.96 [2.34, 5.46]	0.215
Alb (median [IQR]), g/L	25.91 [24.53, 27.30]	25.67 [24.38, 26.89]	26.00 [24.59, 27.37]	0.124	25.69 [24.16, 27.04]	25.58 [24.80, 27.50]	25.75 [24.14, 26.99]	0.465
PTH (median [IQR]), pg/mL	25.97 [18.99, 35.12]	26.49 [18.76, 37.20]	25.24 [19.04, 34.84]	0.393	24.59 [18.66, 32.66]	25.61 [18.60, 32.49]	24.56 [18.74, 33.11]	0.765
Hb (median [IQR]), g/L	90.00 [80.00, 101.00]	88.00 [79.00, 98.00]	90.00 [80.00, 102.00]	0.274	89.00 [80.00, 100.50]	93.00 [83.00, 97.75]	88.00 [78.00, 102.00]	0.487
BNP (median [IQR]), pg/mL	108.00 [65.00, 157.00]	107.00 [68.00, 154.00]	108.00 [65.00, 157.00]	0.883	112.00 [80.00, 153.50]	106.50 [71.25, 142.75]	113.00 [81.00, 157.00]	0.482
UA (median [IQR]), μmol/L	416.00 [373.75, 457.00]	423.00 [378.00, 462.00]	415.00 [371.00, 455.00]	0.379	418.00 [370.50, 467.00]	410.00 [371.00, 450.50]	420.00 [370.00, 469.00]	0.454
Ca (median [IQR]), mmol/L	1.39 [1.07, 1.63]	1.38 [1.15, 1.63]	1.40 [1.05, 1.63]	0.863	1.37 [1.05, 1.65]	1.33 [1.13, 1.65]	1.37 [1.05, 1.65]	0.962
P (median [IQR]), mmol/L	1.06 [0.83, 1.32]	1.00 [0.83, 1.33]	1.08 [0.83, 1.32]	0.656	1.15 [0.90, 1.33]	1.15 [0.86, 1.32]	1.15 [0.94, 1.34]	0.7
NEU (median [IQR]), 10 ⁹ /L	8.83 [7.80, 10.43]	6.85 [6.35, 7.55]	9.78 [8.70, 10.80]	<0.001	9.06 [7.82, 10.57]	7.03 [6.28, 7.49]	9.72 [8.60, 10.71]	<0.001
PLT (median [IQR]), 10 ⁹ /L	123.00 [106.00, 151.00]	225.00 [167.00, 266.00]	113.00 [97.50, 132.50]	<0.001	120.00 [95.00, 144.00]	214.50 [158.00, 258.00]	109.00 [91.00, 133.00]	<0.001
MONO (median [IQR]), 10 ⁹ /L	0.16 [0.09, 0.21]	0.22 [0.16, 0.33]	0.14 [0.07, 0.20]	<0.001	0.16 [0.10, 0.22]	0.31 [0.26, 0.38]	0.15 [0.09, 0.19]	<0.001
LYM (median [IQR]), 10 ⁹ /L	2.42 [1.98, 2.79]	1.53 [1.22, 1.86]	2.63 [2.34, 2.88]	<0.001	2.31 [2.06, 2.75]	1.52 [1.16, 1.76]	2.50 [2.23, 2.83]	<0.001
AISI (median [IQR])	45.05 [29.27, 63.90]	91.90 [73.10, 105.90]	36.40 [22.85, 48.35]	<0.001	40.20 [24.55, 61.05]	94.45 [82.40, 106.70]	34.40 [22.40, 48.60]	<0.001
ASM (median [IQR])	6.09 [4.24, 7.62]	2.92 [2.04, 3.53]	7.03 [5.90, 7.93]	<0.001	6.58 [5.31, 7.39]	3.08 [1.90, 4.00]	7.01 [6.01, 7.59]	<0.001
Contrast (median [IQR])	8.05 [6.62, 9.58]	4.46 [3.23, 5.80]	8.99 [7.91, 9.91]	<0.001	8.66 [7.30, 9.73]	4.03 [3.08, 6.03]	9.17 [8.19, 10.06]	<0.001
Correlation (median [IQR])	7.92 [5.80, 9.02]	4.73 [3.95, 5.39]	8.47 [7.79, 9.40]	<0.001	8.22 [7.03, 9.14]	4.62 [4.22, 5.80]	8.67 [7.97, 9.55]	<0.001
Entropy (median [IQR])	101.00 [79.00, 127.00]	51.00 [29.00, 68.00]	117.00 [96.00, 135.50]	<0.001	105.00 [82.00, 127.50]	46.50 [31.25, 67.00]	116.00 [97.00, 130.00]	<0.001
IDM (median [IQR])	7.45 [5.87, 9.01]	4.70 [3.96, 5.57]	8.38 [7.18, 9.48]	<0.001	7.51 [6.46, 9.26]	4.69 [4.01, 5.34]	8.17 [7.22, 9.54]	<0.001
Energy (median [IQR])	5.10 [3.77, 6.40]	4.85 [3.75, 6.36]	5.17 [3.78, 6.40]	0.335	5.42 [4.06, 6.97]	6.03 [4.10, 7.15]	5.21 [4.05, 6.90]	0.244
SE (median [IQR])	69.00 [46.75, 89.25]	73.00 [50.00, 90.00]	68.00 [45.50, 89.00]	0.34	65.00 [44.00, 93.00]	84.50 [49.00, 103.50]	64.00 [43.00, 87.00]	0.065
DA (median [IQR])	1.24 [1.10, 1.43]	1.29 [1.11, 1.43]	1.22 [1.10, 1.44]	0.445	1.24 [1.09, 1.40]	1.19 [1.11, 1.35]	1.25 [1.09, 1.41]	0.551
DV (median [IQR])	1.44 [0.89, 1.98]	1.35 [0.78, 1.99]	1.47 [0.95, 1.97]	0.371	1.56 [0.94, 2.06]	1.23 [0.78, 1.78]	1.64 [0.98, 2.09]	0.068
IMC (median [IQR])	2.43 [1.92, 2.82]	2.35 [1.88, 2.77]	2.43 [1.94, 2.84]	0.422	2.53 [2.10, 2.99]	2.67 [2.25, 3.06]	2.40 [2.08, 2.96]	0.085

Abbreviations: IQR, interquartile range; BMI, body mass index; eGFR, estimated glomerular filtration rate; Cyst C, cystatin C; UTP, 24-h urinary total protein; Alb, albumin; PTH, Parathyroid hormone; Hb, hemoglobin; BNP, brain natriuretic peptide; UA, uric acid; Ca, calcium; P, phosphorus; NEU, neutrophil count; PLT, platelet count; MONO, monocyte count; LYM, lymphocyte count; AISI, Aggregate Index of Systemic Inflammation; ASM, Angular Second Moment; IDM, Inverse Difference Moment; SE, Sum Entropy; DA, Difference Average; DV, Difference Variance; IMC, Informational Measure of Correlation.

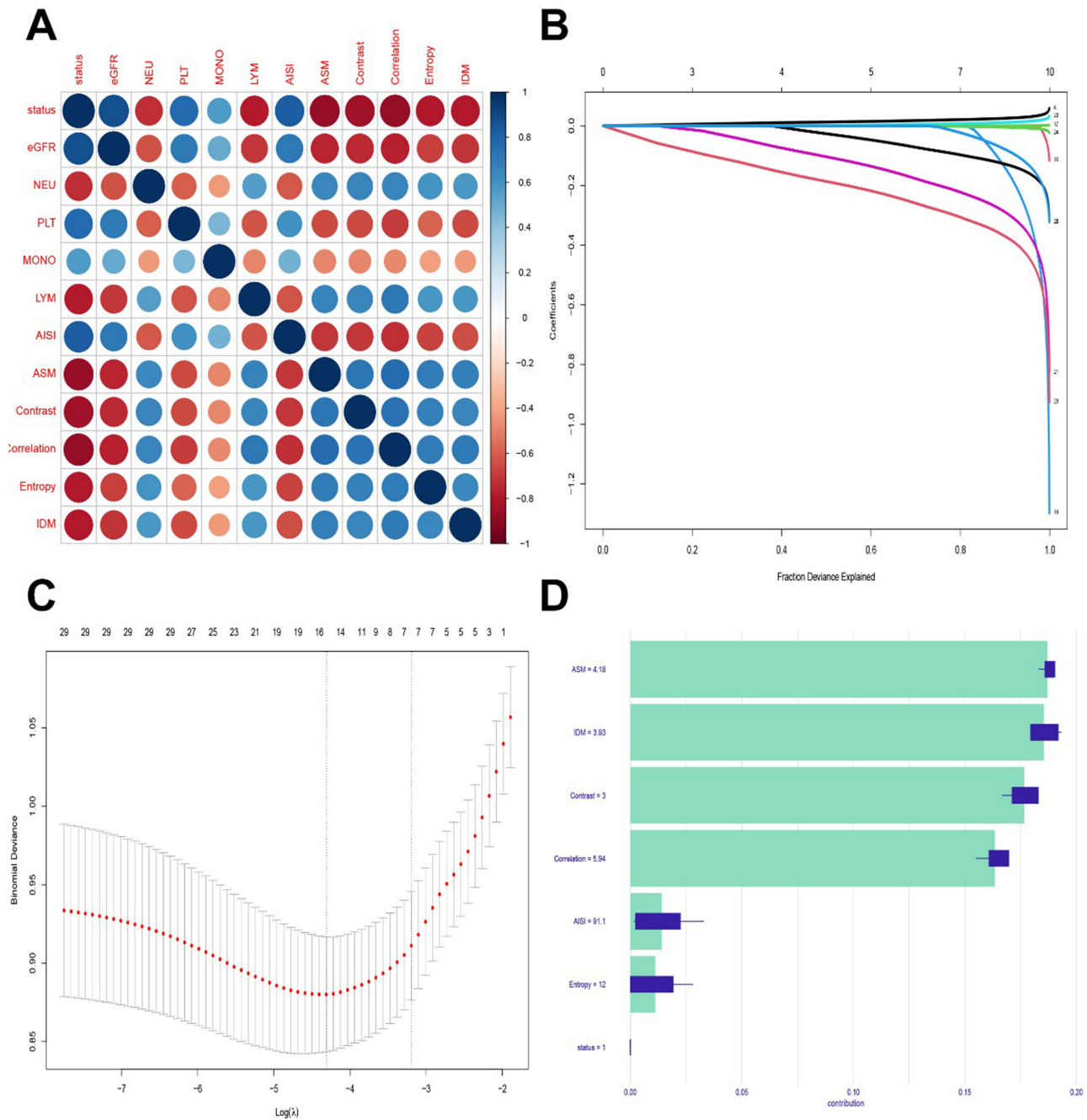


Figure 2 Inclusion and weight analysis of predictive feature factors. **(A)** Pearson coefficient correlation analysis between candidate variables and outcomes. **(B)** Iterative analysis of candidate variables based on Lasso log lambda. **(C)** Ten-fold cross validation based on Lasso regression analysis. **(D)** Comparison of weight values of candidate variables interpretable based on SHAP.

extracted based on the co-occurrence gray matrix, it has shown extremely promising predictive power in becoming a candidate predictor variable.

Comparison of Predictive Performance Across Different Models

We constructed seven ML-based prediction models based on candidate predictor variables. As shown in Table 2, among the candidate variables screened based on logistic regression algorithm, both ultrasound radiomics parameters and AISI were independent risk factors for renal fibrosis ($P < 0.05$). As shown in Table 3 and Figure 3, in the training set, the AUC values of various prediction models ranged from 0.72 (95% CI: 0.67~0.77) to 0.96 (95% CI: 0.92~0.99). In the internal

Table 2 Univariate and Multivariate Logistic Regression Analysis for Independent Risk Factors

Variables	Univariate Logistic Analysis		P-value	Multivariate Logistic Analysis		P-value
	OR	95% CI		OR	95% CI	
AISI	3.56	1.23~5.42	<0.05	3.29	1.01~4.89	<0.05
ASM	2.05	0.86~3.27	<0.05	2.08	0.78~3.68	<0.05
Contrast	1.87	0.26~3.04	<0.05	1.99	0.31~3.42	<0.05
Correlation	2.16	1.02~4.22	<0.05	2.25	0.99~3.84	<0.05
Entropy	1.06	0.64~2.99	<0.05	1.34	0.71~3.05	<0.05
IDM	1.13	0.54~2.87	<0.05	1.26	0.51~2.76	<0.05

Abbreviations: OR, odds ratio; 95% CI, 95% confidence interval; AISI, Aggregate Index of Systemic Inflammation; ASM, Angular Second Moment; IDM, Inverse Difference Moment.

Table 3 Predictive Performance Comparison of the Seven Types of ML Algorithms

Prediction Model	Training Set				Internal Set				External Set			
	AUC	95% CI	PPV	NPV	AUC	95% CI	PPV	NPV	AUC	95% CI	PPV	NPV
EGE	0.79	0.73~0.84	0.78	0.97	0.78	0.73~0.83	0.78	0.95	0.78	0.73~0.83	0.78	0.95
SVM	0.89	0.83~0.94	0.92	0.99	0.85	0.79~0.91	0.92	0.99	0.86	0.81~0.91	0.88	0.95
RF	0.96	0.92~0.99	0.96	0.99	0.93	0.88~0.98	0.96	0.99	0.95	0.89~0.99	0.95	0.99
MP	0.87	0.81~0.92	0.88	0.98	0.82	0.77~0.87	0.86	0.95	0.84	0.78~0.89	0.80	0.95
ANN	0.83	0.78~0.88	0.86	0.98	0.81	0.76~0.86	0.82	0.96	0.81	0.76~0.86	0.78	0.92
NB	0.77	0.72~0.82	0.76	0.97	0.75	0.70~0.80	0.75	0.95	0.75	0.70~0.80	0.75	0.95
GLR	0.72	0.67~0.77	0.68	0.95	0.71	0.66~0.76	0.70	0.92	0.69	0.64~0.74	0.70	0.85

Abbreviations: AUC, Area under the curve; 95% CI, 95% confidence interval; PPV, Positive predictive value; NPV, negative predictive value; EGE, extreme gradient enhancement; SVM, support vector machine; RF, random forest; MP, multilayer perceptron; ANN, artificial neural network; NB, naive Bayes; GLR, generalized linear logistic regression.

test set, the AUC values of various prediction models ranged from 0.71 (95% CI: 0.66~0.76) to 0.93 (95% CI: 0.88~0.98). Among them, the AUC values of the prediction model based on RF algorithm in the training set and internal validation set were 0.96 (95% CI: 0.92~0.99) and 0.93 (95% CI: 0.88~0.98), respectively, while the prediction model GLR with the worst prediction performance had AUC values of 0.72 (95% CI: 0.67~0.77) and 0.71 (95% CI: 0.66~0.76) in the training set and internal validation set, respectively. In addition, the AUC value of RF in the external test set can still reach AUC values of 0.95 (95% CI: 0.89~0.99). Moreover, as shown in [Figure 4](#), in the DCA evaluation of the net benefits of various prediction models, the prediction model constructed by the RF algorithm still has the best net benefit, indicating that among the seven ML constructed renal fibrosis prediction models, RF can become the best prediction model for predicting renal fibrosis.

Performance Evaluation of the RF Model on the External Cohort

After 1000 resampling times, as shown in [Figure 5](#), RF demonstrated satisfactory robustness in all three datasets (the C-index is between 0.99 and 1.00). Then, as shown in [Supplementary Table 3](#), since both the ultrasound radiomics parameters and AISI are assigned quantization values in the RF algorithm, the calculation formula of the RF prediction model is as follows: $RF(x) = \underset{k}{\operatorname{argmax}} \sum_{i=1}^n I(y_i = k)$. Among them, n is the number of decision trees in the random forest, and k is regarded as the included predictor variable parameter. As shown in [Figure 6](#) and [Supplementary Figure 1](#), the discriminative efficacy of the renal fibrosis prediction model constructed based on the RF algorithm is excellent in the training set, internal and external test sets. Collectively, the renal fibrosis prediction model constructed based on RF has extremely significant clinical application value and generalization ability.

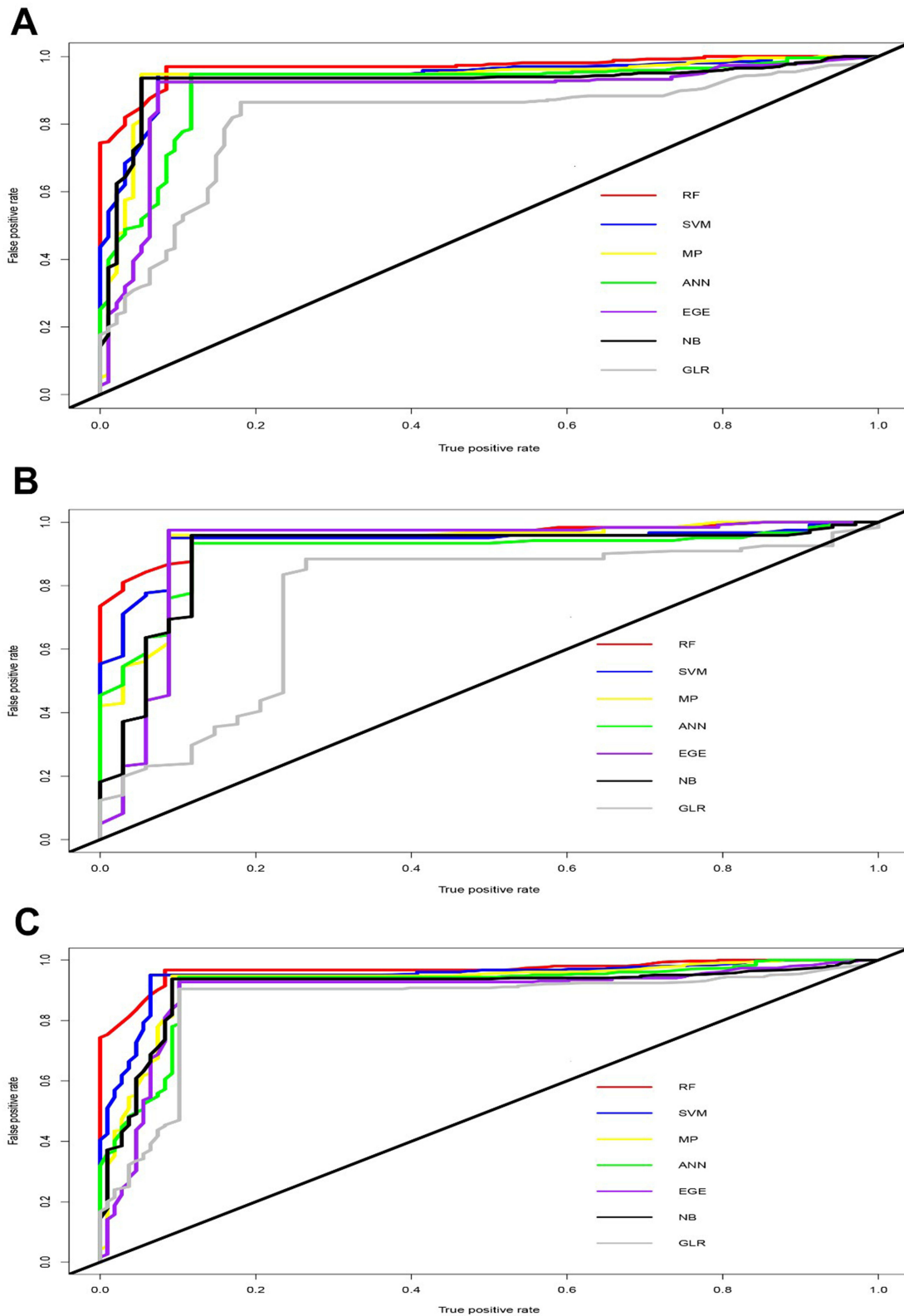


Figure 3 Evaluation of ROC for ML-based prediction model. The AUC values of 7 prediction models for the (A) Training set and (B) Internal validation set (C) External validation set.

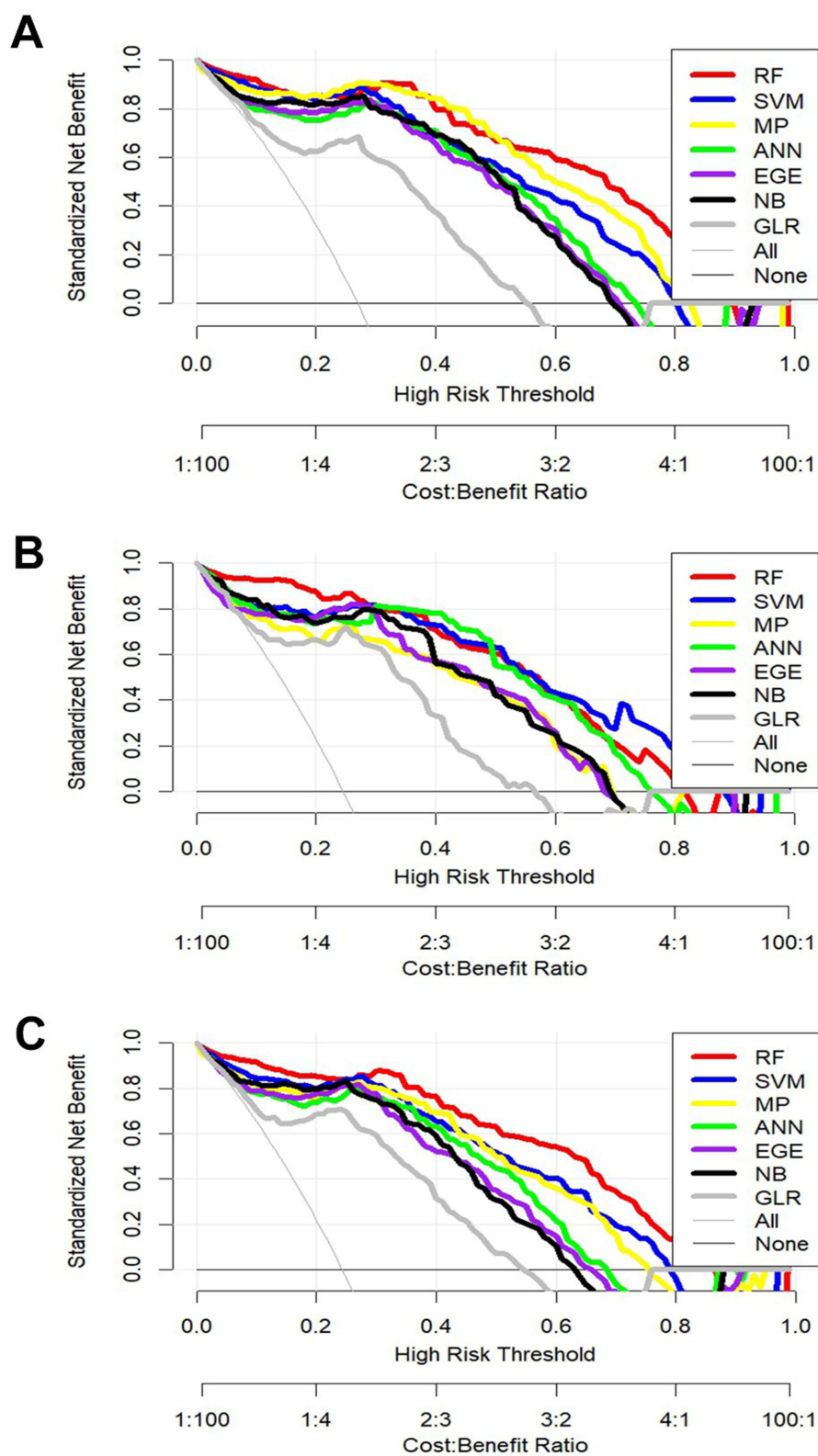


Figure 4 Evaluation of DCA for ML-based prediction model. The DCA of 7 prediction models for the (A) Training set and (B) Internal validation set (C) External validation set.

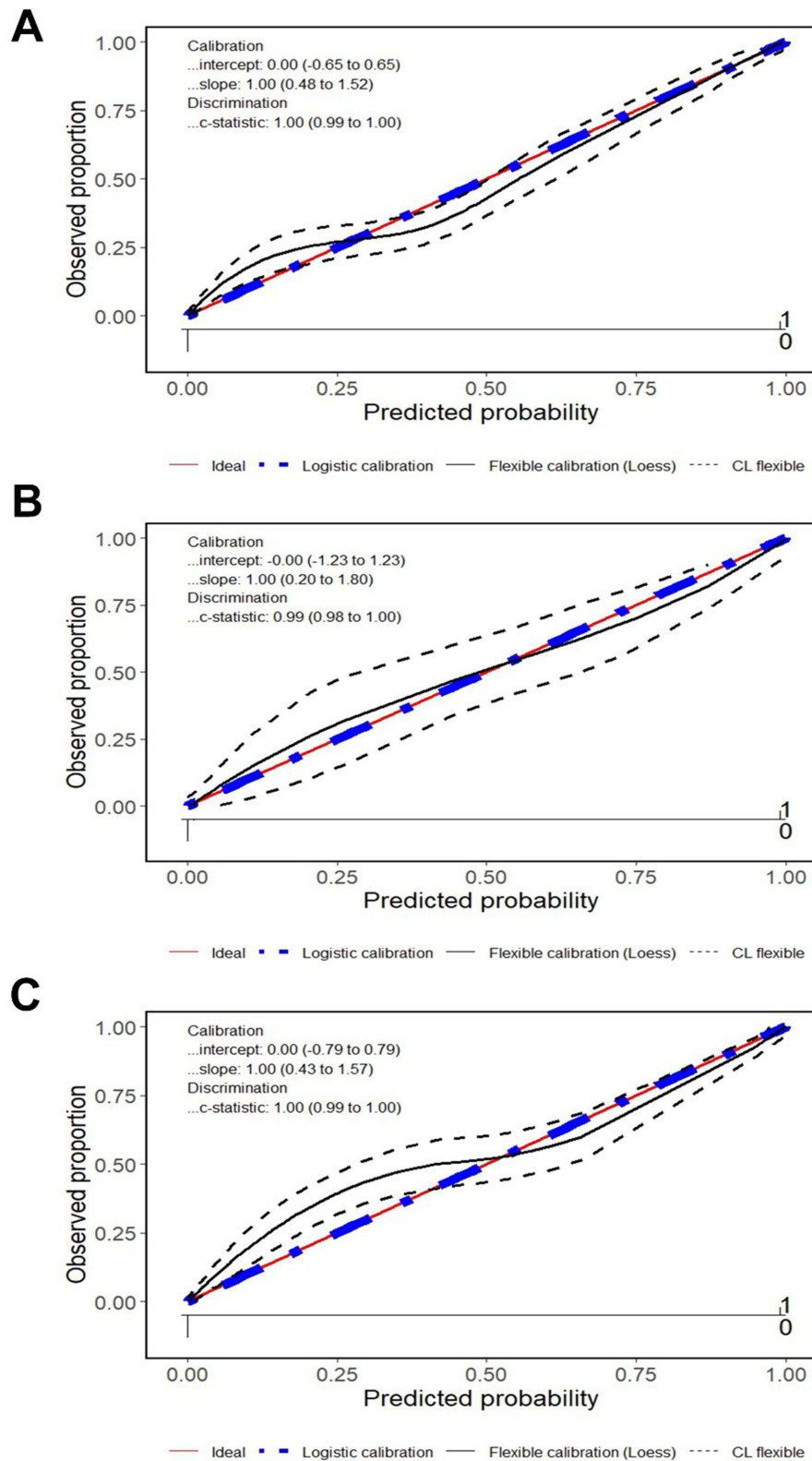


Figure 5 Evaluation of calibration curve for RF prediction model. The calibration curve after 1000 bootstrap for the (A) Training set; (B) Internal validation set; (C) External validation set.

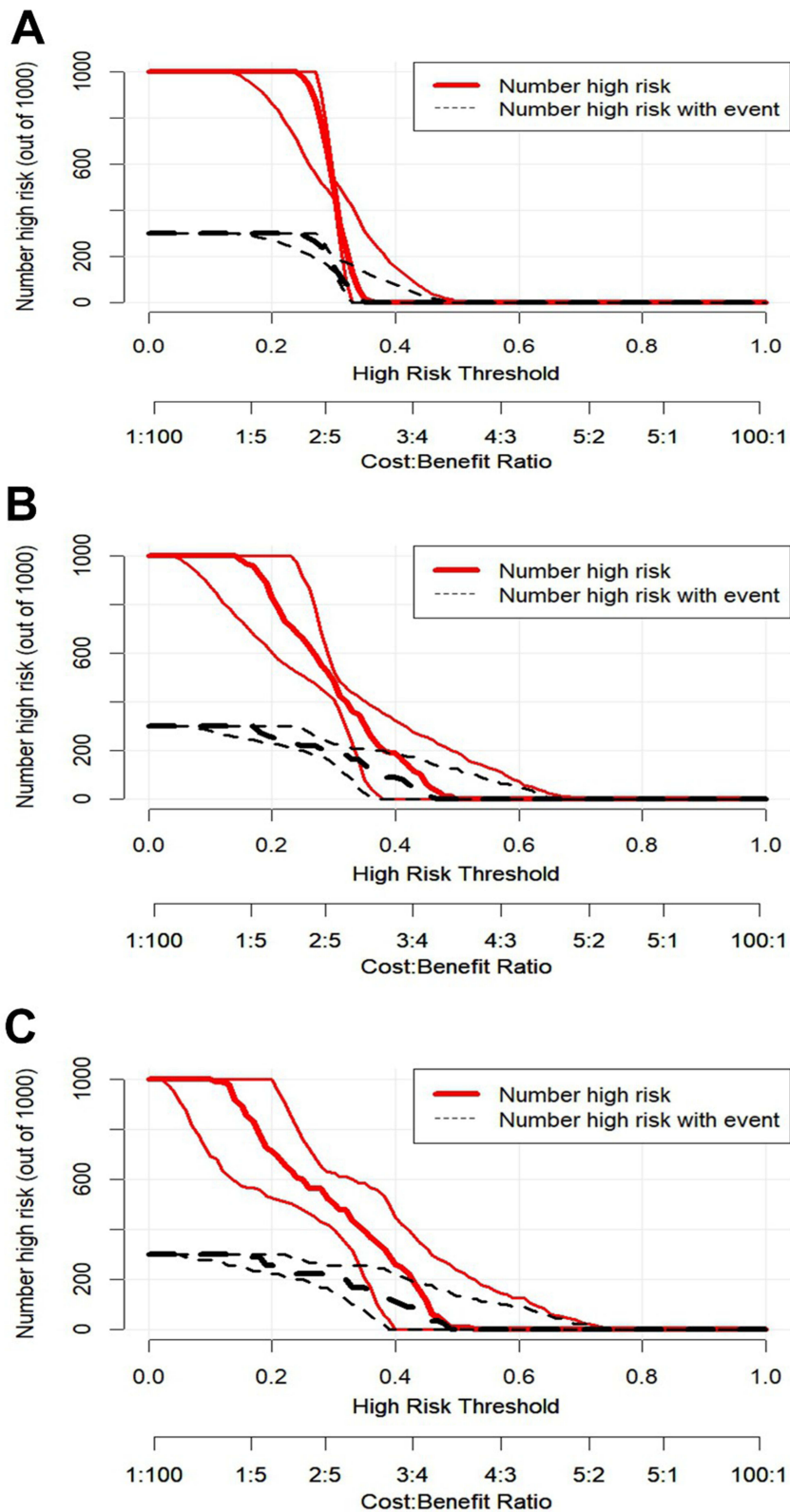


Figure 6 Evaluating the efficacy of RF in clinical applications based on CIC. (A) Training set; (B) Internal validation set; (C) External validation set.

Discussion

CKD, as a chronic progressive disease, is expected to pose a health and medical burden to 10% to 14% of the global population worldwide.^{23–25} As CKD progresses, renal fibrosis, as a hallmark manifestation of different progressive CKD, is characterized by excessive deposition of extracellular matrix leading to scar formation.²⁶ Cautiously, as the degree of renal injury progresses, progressive loss of glomerular capillary structure, tubular atrophy and narrowing, and replacement of glomerular cellular components by expanded extracellular matrix and fibrous tissue lead to a decrease in glomerular effective filtration area and eGFR.^{27,28} The degree of IF/TA indicates the loss of functional nephrons and the progression of renal injury.⁶ Normally, patients with CKD are often accompanied by endothelial damage, vascular calcification, hypertension, and peripheral arterial disease, which are closely related to the development of end-stage renal disease and the occurrence of cardiovascular disease.^{29,30} Hypertension is the main cause of CKD progression and persistent vascular disease.³ In this study, significant differences were found in eGFR and mean arterial pressure among CKD patients with different levels of IF/TA, indicating that as the degree of renal fibrosis increases, the risk of renal dysfunction and cardiovascular disease also increases. In view of this, non-invasive and accurate assessment of the degree of IF/TA is of great clinical significance in the selection of treatment plans and prognosis evaluation for patients with CKD.

Non invasive assessment of the degree of fibrosis in CKD has always been regarded as an urgent need in current clinical diagnosis and treatment, and radiomics based on ultrasound images has the potential to meet this demand. For example, Huang et al extracted ultrasound feature parameters through multimodal ultrasound, particularly based on shear wave elastography, and angio planewave ultrasensitive imaging characteristics.¹⁴ The constructed prediction model has an AUC value of over 0.7 in predicting CKD related renal fibrosis, indicating that ultrasound parameters have certain advantages in predictive performance. In addition, Chen et al also constructed a renal fibrosis prediction model using Ultrasonic renal length. However, renal length presented limited discrimination ability in distinguishing degrees of renal fibrosis while controlling the key confounding factors, yielding an area under the ROC curve of only 0.58 (95% CI 0.45–0.70).¹⁵ Previous studies have shown that ultrasound affects the efficacy and robustness of omics in predicting renal fibrosis, which may be closely related to the parameters extracted by ultrasound and the algorithms used to construct prediction models.^{9,15,31} In addition, due to the inability of small sample queues to generalize predictive models, continuous optimization is still needed for the exploration of ultrasound radiomics. In this study, we extracted a large number of ultrasound imaging parameters based on convolutional neural networks, and screened reliable ultrasound imaging omics prediction candidate parameters based on multiple iterations. The optimal AUC values of 0.96 and 0.95 were obtained in the training and validation sets, respectively. Therefore, the renal fibrosis prediction model constructed based on ultrasound parameters and ML algorithms has great clinical application value.

AISI, as an easily accessible indicator and a novel prognostic biomarker, AISI has been used to predict patients with idiopathic pulmonary fibrosis (IPF).²¹ Previous studies have shown that it can significantly distinguish between IPF patients and healthy subjects, and AISI levels are independently associated with poor prognosis.^{21,32} In addition, research should also demonstrate a significant correlation between AISI and poor prognosis in patients with viral pneumonia.¹⁹ However, few studies have investigated the predictive value of AISI for renal fibrosis outcomes.

Previous studies have shown that AISI is significantly positively correlated with the incidence of CKD and has better predictive power compared to other inflammatory indicators.²² Consistent with previous research findings, our study found that the AUC for predicting renal fibrosis based on AISI independent indicators was 0.88 and 0.89 in the training and validation sets, respectively. We speculate that perivascular cells are now considered the main innate immune sentinels in the kidneys, producing pro-inflammatory cytokines and chemokines after injury. These mediators promote immune cell infiltration, leading to persistent inflammation and progression of renal fibrosis.³³ Therefore, the interactions between perivascular cells and renal tubular epithelial cells, immune cells, and endothelial cells are key processes in physiological and pathophysiological states.

Although ML models have been proven to achieve high accuracy in clinical applications, the impact of individual variables on these models is often still unknown.³⁴ This lack of transparency limits the application of ML in clinical practice. In this study, we performed SHAP interpretability weight ranking on ultrasound imaging parameters and AISI. By combining optimal credit allocation with local interpretation, we intuitively represented the importance of each variable in the model, providing more interpretable outputs. More importantly, in the RF prediction model constructed using ultrasound radiomics combined with AISI, the AUC values for predicting renal fibrosis in the training and internal validation sets were 0.96 and

0.95, respectively, indicating that the combined parameters and ML can achieve better prediction performance. The predictive model constructed by Wu et al using RF algorithm combined with serum creatinine based approach has a predictive performance AUC value of 0.89, which is consistent with the results of this study.³⁵ This indicates that RF algorithm is suitable for constructing renal fibrosis prediction models. However, the selection of candidate variables directly determines the predictive performance and superiority of RF algorithm.

This research also inevitably has the following limitations. Firstly, as a retrospective study, selection bias is inevitable in the collection of patients' clinical data and ultrasound images. Notably, substandard-quality ultrasound images could not be utilized, directly leading to the loss of patient information. To address this, future prospective randomized controlled trials are needed for compensation, with stricter inclusion criteria to minimize data loss. Secondly, although internal and external tests of the prediction model were conducted using data from two tertiary hospitals, the generalization ability and generalizability of the model still require repeated verification through large-sample, multi-center cohort studies. Additionally, inter-operator variability in ultrasound examinations may affect radiomic feature extraction. Although our center implemented standardized training for sonographers and regularly assessed inter-observer agreement (with a kappa coefficient of 0.82, indicating good consistency), differences in operational proficiency across different institutions may still impact model performance. Thirdly, this study incorporated ultrasound imaging parameters and albumin-to-iron ratio to construct the renal fibrosis predictive model. However, for non-invasive diagnostic models, it is necessary to continue exploring candidate markers with potential value, such as uromics and MRI radiomics. In summary, the goal is to identify optimal, convenient, and cost-effective predictive factors for clinical application. Regarding clinical implications, to enhance the practicality of the model, we suggest integrating it with portable ultrasound devices, which can facilitate its use in resource-limited settings, enabling more widespread screening and monitoring of chronic kidney disease patients.

Conclusion

In summary, we developed a RF model based on ML algorithms that combines ultrasound radiomics parameters and AISI to evaluate renal fibrosis. Their integration is a key innovation, with synergistic effects enhancing diagnostic performance. The model achieved a superior AUC of 0.96 in the training set, outperforming conventional methods. The included ultrasound radiomics parameters and AISI are easy to obtain, with high diagnostic value, good reproducibility, economy and cost-effectiveness, and they do not increase patients' medical burden. Specifically, for high-risk renal fibrosis patients, this RF model enables dynamic evaluation of renal fibrosis and assists in pre-biopsy decision-making. It provides a practical non-invasive alternative with potential for wide clinical application to improve the efficiency and accuracy of renal fibrosis assessment.

Disclosure

The authors report no conflicts of interest in this work.

References

1. KDIGO. 2024 clinical practice guideline for the evaluation and management of chronic kidney disease. *Kidney Int.* 2024;105(4s):S117–s314. doi:10.1016/j.kint.2023.10.018
2. Bello AK, Okpechi IG, Levin A, et al. An update on the global disparities in kidney disease burden and care across world countries and regions. *Lancet Glob Health.* 2024;12(3):e382–e95. doi:10.1016/S2214-109X(23)00570-3
3. Jankowski J, Floege J, Fliser D, Böhm M, Marx N. Cardiovascular disease in chronic kidney disease: pathophysiological insights and therapeutic options. *Circulation.* 2021;143(11):1157–1172. doi:10.1161/CIRCULATIONAHA.120.050686
4. Schuett K, Marx N, Lehrke M. The cardio-kidney patient: epidemiology, clinical characteristics and therapy. *Circ Res.* 2023;132(8):902–914. doi:10.1161/CIRCRESAHA.122.321748
5. Jia YY, Yu Y, Li HJ. The research status and prospect of periostin in chronic kidney disease. *Renal Failure.* 2020;42(1):1166–1172. doi:10.1080/0886022X.2020.1846562
6. Tampe D, Schridde L, Korsten P, et al. Different patterns of kidney fibrosis are indicative of injury to distinct renal compartments. *Cells.* 2021;10(8):2014. doi:10.3390/cells10082014
7. Bullen AL, Vaingankar S, Madero M, et al. Urine uromodulin, kidney tubulointerstitial fibrosis, and furosemide response. *Nephron.* 2024;148(7):443–447. doi:10.1159/000534578
8. Poggio ED, McClelland RL, Blank KN, et al. Systematic review and meta-analysis of native kidney biopsy complications. *Clin J Am Society Nephrol.* 2020;15(11):1595–1602. doi:10.2215/CJN.04710420
9. Cè M, Felisaz PF, Ali M, Sartò GV R, Cellina M. Ultrasound elastography in chronic kidney disease: a systematic review and meta-analysis. *J Med Ultrasonics.* 2023;50(3):381–415. doi:10.1007/s10396-023-01304-z

10. Ng KH, Wong JHD, Leong SS. Shear wave elastography in chronic kidney disease - the physics and clinical application. *Phys Eng Sci Med.* 2024;47(1):17–29. doi:10.1007/s13246-023-01358-w
11. Bob F, Grosu I, Spore I, et al. Is kidney stiffness measured using elastography influenced mainly by vascular factors in patients with diabetic kidney disease? *Ultrasonic Imaging.* 2018;40(5):300–309. doi:10.1177/0161734618779789
12. Sohn JH, Fields BKK. Radiomics and deep learning to predict pulmonary nodule metastasis at CT. *Radiology.* 2024;311(1):e233356. doi:10.1148/radiol.233356
13. Li Y, Lyu B, Wang R, et al. Machine learning-based radiomics to distinguish pulmonary nodules between lung adenocarcinoma and tuberculosis. *Thoracic Cancer.* 2024;15(6):466–476. doi:10.1111/1759-7714.15216
14. Huang X, Wei T, Li J, et al. Multimodal ultrasound for assessment of renal fibrosis in biopsy-proven patients with chronic kidney disease. *Ultraschall in der Medizin.* 2025. doi:10.1055/a-2559-7743
15. Chen Z, Jiang J, Gunda ST, et al. Ultrasonic renal length as an indicator of renal fibrosis severity in non-diabetic patients with chronic kidney disease. *Clin Experi Nephrol.* 2025;29(4):460–468. doi:10.1007/s10157-024-02598-0
16. Okda HI, Keshk RAE, El-Anwar N, El Behiry AM, Gamaleldin SM. The role of strain wave elastography in the evaluation of renal fibrosis in patients with kidney diseases. *Nefrologia.* 2025;45(3):259–270. doi:10.1016/j.nefro.2024.10.007
17. Tuzimek A, Dzedzic EA, Beck J, Kochman W. Correlations between acute coronary syndrome and novel inflammatory markers (Systemic immune-inflammation index, systemic inflammation response index, and aggregate index of systemic inflammation) in patients with and without diabetes or prediabetes. *J Inflamm Res.* 2024;17:2623–2632. doi:10.2147/JIR.S454117
18. Xiu J, Lin X, Chen Q, et al. The aggregate index of systemic inflammation (AISI): a novel predictor for hypertension. *Front Cardiovasc Med.* 2023;10:1163900. doi:10.3389/fcvm.2023.1163900
19. Hosseninia S, Ghobadi H, Garjani K, Hosseini SAH, Aslani MR. Aggregate index of systemic inflammation (AISI) in admission as a reliable predictor of mortality in COPD patients with COVID-19. *BMC Pulm Med.* 2023;23(1):107. doi:10.1186/s12890-023-02397-5
20. Ghobadi H, Mohammadshahi J, Javaheri N, Fouladi N, Mirzazadeh Y, Aslani MR. Role of leukocytes and systemic inflammation indexes (NLR, PLR, MLP, dNLR, NLPR, AISI, SIR-I, and SII) on admission predicts in-hospital mortality in non-elderly and elderly COVID-19 patients. *Front Med.* 2022;9:916453. doi:10.3389/fmed.2022.916453
21. Zinellu A, Collu C, Nasser M, et al. The Aggregate Index of Systemic Inflammation (AISI): a novel prognostic biomarker in idiopathic pulmonary fibrosis. *J Clin Med.* 2021;10(18):4134. doi:10.3390/jcm10184134
22. Huang D, Wu H. Association between the aggregate index of systemic inflammation and CKD: evidence from NHANES 1999–2018. *Front Med.* 2025;12:1506575. doi:10.3389/fmed.2025.1506575
23. Fletcher BR, Damery S, Aiyegbusi OL, et al. Symptom burden and health-related quality of life in chronic kidney disease: a global systematic review and meta-analysis. *PLoS Med.* 2022;19(4):e1003954. doi:10.1371/journal.pmed.1003954
24. Zhao WM, Li XL, Shi R, et al. Global, regional and national burden of CKD in children and adolescents from 1990 to 2019. *Nephrol Dial Transplant.* 2024;39(8):1268–1278. doi:10.1093/ndt/gfad269
25. Song J, Pan T, Xu Z, et al. A systematic analysis of chronic kidney disease burden attributable to lead exposure based on the global burden of disease study 2019. *Sci Total Environ.* 2024;908:168189. doi:10.1016/j.scitotenv.2023.168189
26. McDonnell T, Banks RE, Taal MW, Vuilleumier N, Kalra PA. Personalized care in CKD: moving beyond traditional biomarkers. *Nephron.* 2025;2025:1–19.
27. Huang R, Fu P, Ma L. Kidney fibrosis: from mechanisms to therapeutic medicines. *Signal Transduct Target Ther.* 2023;8(1):129. doi:10.1038/s41392-023-01379-7
28. Panizo S, Martínez-Arias L, Alonso-Montes C, et al. Fibrosis in chronic kidney disease: pathogenesis and consequences. *Int J Mol Sci.* 2021;22(1):408. doi:10.3390/ijms22010408
29. Banerjee D, Rosano G, Herzog CA. Management of heart failure patient with CKD. *Clin J Am Society Nephrol.* 2021;16(7):1131–1139. doi:10.2215/CJN.14180920
30. Szlagor M, Dybiec J, Młynarska E, Rysz J, Franczyk B. Chronic kidney disease as a comorbidity in heart failure. *Int J Mol Sci.* 2023;24(3):2988. doi:10.3390/ijms24032988
31. Qin X, Liu X, Xia L, Luo Q, Zhang C. Multimodal ultrasound deep learning to detect fibrosis in early chronic kidney disease. *Renal Failure.* 2024;46(2):2417740. doi:10.1080/0886022X.2024.2417740
32. Zinellu A, Paliogiannis P, Sotgiu E, et al. Blood cell count derived inflammation indexes in patients with idiopathic pulmonary fibrosis. *Lung.* 2020;198(5):821–827. doi:10.1007/s00408-020-00386-7
33. Tanaka S, Portilla D, Okusa MD. Role of perivascular cells in kidney homeostasis, inflammation, repair and fibrosis. *Nat Rev Nephrol.* 2023;19(11):721–732. doi:10.1038/s41581-023-00752-7
34. Cabitza F, Rasoini R, Gensini GF. Unintended consequences of machine learning in medicine. *JAMA.* 2017;318(6):517–518. doi:10.1001/jama.2017.7797
35. Wu LH, Zhao D, Niu JY, et al. Development and validation of multi-center serum creatinine-based models for noninvasive prediction of kidney fibrosis in chronic kidney disease. *Renal Failure.* 2025;47(1):2489715. doi:10.1080/0886022X.2025.2489715

International Journal of General Medicine

Publish your work in this journal

The International Journal of General Medicine is an international, peer-reviewed open-access journal that focuses on general and internal medicine, pathogenesis, epidemiology, diagnosis, monitoring and treatment protocols. The journal is characterized by the rapid reporting of reviews, original research and clinical studies across all disease areas. The manuscript management system is completely online and includes a very quick and fair peer-review system, which is all easy to use. Visit <http://www.dovepress.com/testimonials.php> to read real quotes from published authors.

Submit your manuscript here: <https://www.dovepress.com/international-journal-of-general-medicine-journal>

Dovepress
Taylor & Francis Group